

Molecular dynamics study of the surface melting of iron clusters

F. Ding^a, K. Bolton, and A. Rosén

Experimental Physics, School of Physics and Engineering Physics, Göteborg University and Chalmers University of Technology, 412 96 Göteborg, Sweden

Received 6 September 2004

Published online 13 July 2005 – © EDP Sciences, Società Italiana di Fisica, Springer-Verlag 2005

Abstract. Molecular dynamics simulations have been used to study the surface melting of iron clusters. It is found that, even when the temperature is several hundreds of Kelvin below the cluster melting point, the crystalline center of the cluster is surrounded by surface atoms that exhibit large amplitude diffusion from their original positions. This results in surface melting of the cluster.

PACS. 31.15.Qg Molecular dynamics and other numerical methods – 36.40.Ei Phase transitions in clusters

Introduction

Nanometer clusters or nanoparticles have been the focus of interest in recent years because of their unique physical and chemical properties, as well as their potential application in a diverse range of new materials, electronic-devices and chemical sensors [1]. In contrast to bulk materials, the properties of nano-materials are often correlated to their large fraction of surface atoms, or their high surface:volume ratio. Recently, carbon nanotubes (CNTs) [2] and carbon fibers (CFs) [3] have been produced by catalytic chemical vapor deposition (CCVD) at temperatures far below the melting point of the catalyst particles. Under these conditions it has been proposed that diffusion of the C atoms on the cluster surface is important for the CF and CNT nucleation [4].

Although surface melting is very important, the detail mechanism has not been as well studied as bulk melting of metal clusters. In this paper we report MD studies of the surface melting of iron clusters. Analysis of the Lindemann index for the cluster and each cluster atom shows the existence of a molten surface state at temperatures well below the melting point of the cluster.

1 Potential energy surface and simulation methods

Previous investigations have shown that the many-body interaction potential, which is based on the second moment approximation of the tight binding model [4,5] is suitable for studying the thermal properties of the pure [6–9] and alloy [10] transition metal systems. The interaction energy between iron atoms can be written as

a sum of Born-Mayer type repulsive energies and many-body attractive energies as:

$$E = \sum_{i \neq j} A \exp \left[-p \left(\frac{r_{ij}}{r_0} - 1 \right) \right] - \sum_i \left\{ \sum_j \xi^2 \exp \left[-2q \left(\frac{r_{ij}}{r_0} - 1 \right) \right] \right\}^{1/2},$$

where r_{ij} is the distance between the i th and j th iron atoms. The parameters $A = 0.13315$ eV, $\xi = 1.6179$ eV, $p = 10.50$, $q = 2.60$ and $r_0 = 2.553$ Å are taken from reference [10].

In the studies presented here the constant temperature molecular dynamics (CTMD) technique was used to study the thermal properties of Fe₅₈₆ clusters (i.e., the Fe cluster has 586 atoms). Studies of clusters of different sizes show similar results to those presented here. In these studies the Fe₅₈₆ cluster initially has a perfect Wulff polyhedral structure (Fig. 1a) which is very stable [11]. The thermal properties of the cluster were studied by heating the cluster from 600 to 1400 K in steps of 50 K. The temperature was controlled by the Berendsen scaling method and the integration time step was 2 fs. 5×10^5 MD trajectory steps were propagated at each temperature, which is sufficient to ensure the validity of the results presented here (doubling the integration time did not change the results). The Lindemann indices [12] of each atom and of the entire cluster were calculated at each temperature as:

$$\delta_i = \frac{1}{N-1} \sum_{j(\neq i)} \frac{\sqrt{\langle r_{ij}^2 \rangle_T - \langle r_{ij} \rangle_T^2}}{\langle r_{ij} \rangle_T}$$
$$\delta = \frac{1}{N} \sum_i \delta_i,$$

^a e-mail: fengding@fy.chalmers.se

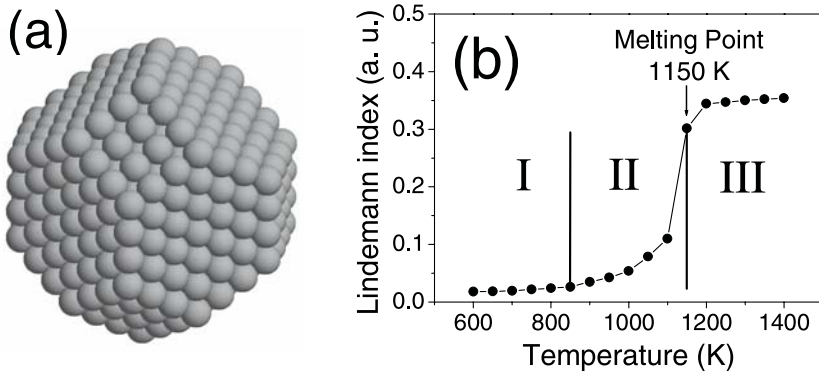


Fig. 1. (a) Initial structure of the Fe₅₈₆ Wulff polyhedral cluster. (b) Lindemann index vs. temperature during the melting of this cluster.

where δ_i and δ are the Lindemann indices of i th atom and the cluster, respectively, $\langle \dots \rangle_T$ denotes the thermal average at temperature T , r_{ij} is the distance between the i th and j th atoms and $N = 586$ is the number of atoms in the system.

2 Results and discussion

Figure 1b shows the temperature dependence of the Lindemann index of the cluster, obtained at each of the 50 K intervals during heating. It is evident that the melting point of the cluster is 1150 K. It is also clear from the figure that the melting process can be divided into three stages. In the first stage, where the temperature is lower than 850 K, the Lindemann index increases slowly and linearly with temperature. During the second stage (850–1150 K) the increase in the Lindemann index is rapid (compared to the first stage) and non-linear. The third stage is the high temperature region where the cluster is completely (bulk) melted and the value of Lindemann index reaches a maximum of about 0.35.

The linear increase in the Lindemann index during the first, low temperature stage is due to the linear increase in atomic kinetic energy with temperature. The value of the Lindemann index during this stage is very small since most of the cluster atoms, including those in the central part and on the surface, do not have large amplitude motion but merely vibrate around their original lattice positions. That is, the cluster is solid at these temperatures.

Surface melting (or diffusion) occurs in the initial part of the second stage. At these temperature, the atoms in the central part of the cluster remain near their original positions in the Wulff polyhedral lattice structure, whereas the surface atoms diffuse away from their initial lattice sites. Hence, when the temperature is higher than 850 K the surface atoms have sufficient kinetic energy to overcome the binding energy at the surface sites (which have a lower coordination than the lattice sites in the center of the cluster) and they can diffuse along the surface. There is therefore a large increase in the Lindemann index of these atoms (discussed below) and of the cluster (Fig. 1b).

Figure 2 shows the radial distribution of the Lindemann indices for all atoms in the Fe₅₈₆ cluster (the distance of each atom from the cluster center of mass —

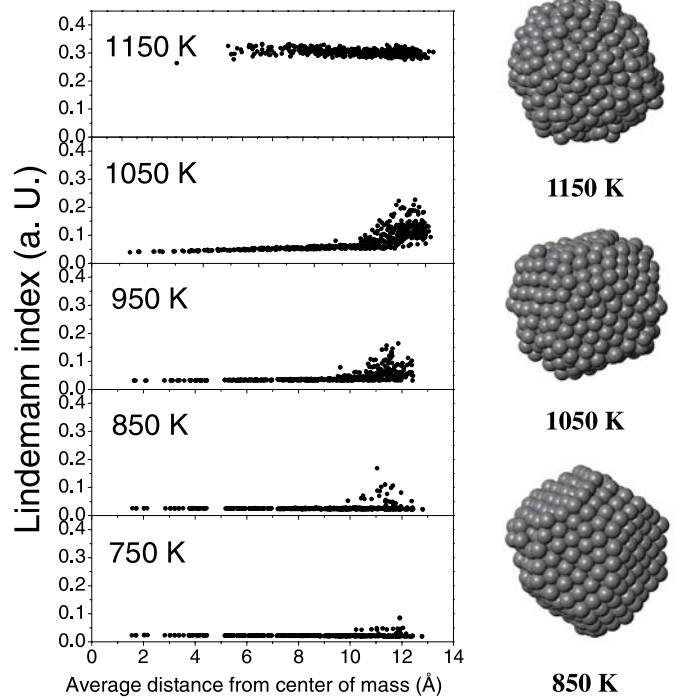


Fig. 2. Radial distribution of the Lindemann indices of the atoms in the Fe₅₈₆ cluster at different temperatures (left panel) and snapshots of the cluster at different temperatures showing the surface melting (right panel).

shown on the x -axis — is the average distance obtained over the trajectory). At temperatures below the melting point (1150 K) the atoms on the cluster surface have larger Lindemann indices than those near the center, which confirms the fact that the surface atoms have large amplitude diffusion away from their original lattice positions whereas the central atoms remain near their lattice positions. It is also evident that an increase in temperature leads to an increase in the number of surface atoms that diffuse from their lattice positions, i.e., an increase in temperature leads to an increase in surface diffusion or surface melting. This is illustrated in Figure 3 where the number of surface atoms that have a high mobility (somewhat arbitrarily defined as atoms that have a Lindemann index larger than 0.1) is plotted as a function of temperature.

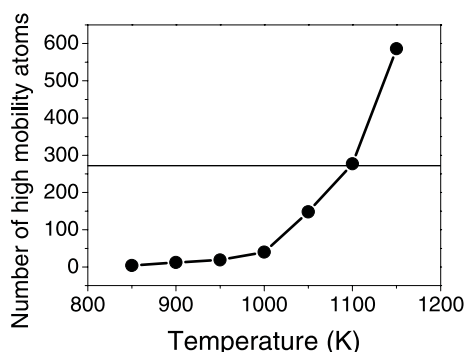


Fig. 3. Temperature dependence of number of cluster atoms that have large amplitude motion (defined as those atoms with Lindemann indices larger than 0.1) in the Fe_{586} cluster during the melting process. The horizontal solid line shows the number of surface atoms in the Fe_{586} Wulff polyhedral cluster.

At 1050 and 1100 K more than half of the cluster atoms exhibit large amplitude diffusion. At the melting point, 1150 K, there is a sudden collapse of the crystal structure and all of the cluster atoms have large Lindemann indices.

The right panel in Figure 2 shows snapshots of the cluster at different temperatures. It is clear that there is an increase in surface disorder with increasing temperature. It may also be noted that at 1050 K, which is just 100 K below the melting point, atoms in the central part of the cluster are still in the fcc solid state. Hence, these solid particles consist of a solid center that is surrounded by surface atoms that undergo large amplitude diffusion. This is surface melting of solid nanoscale particles, as has been proposed previously [13].

It can also be noted that the quantitative features (e.g., the width) of the surface melting that are observed in the short time simulations are not directly related to the surface melting that is expected under experimental conditions. However, the results presented in this contribution (i.e., the presence in a surface molten layer and the increase in width of the layer with increasing temperature) are expected to be valid under experimental conditions. This type of surface melting can be seen, for example, by the continually changing shape of metal clusters that are used as catalysts in CF growth [14].

3 Conclusion

In conclusion, surface melting of the clusters below their melting point has been studied using MD simulation and determining the atomic and cluster Lindemann indices. Surface melting occurs at temperatures that are several hundreds of Kelvin below the cluster melting point. The width of the surface molten layer increases with increasing temperature, and at the melting point there is a sudden collapse of the cluster lattice structure and all atoms show large amplitude diffusion.

We are grateful to the Swedish Foundation for Strategic Research (CAMEL consortium) and the Swedish Research Council for financial support, and for time allocated on the Swedish National Supercomputing facilities.

References

1. S. Link, M.A. El-Sayed, *Annu. Rev. Phys. Chem.* **54**, 331 (2003)
2. S. Hofmann, C. Ducati, J. Robertson, B. Kleinsorge, *App. Phys. Lett.* **83**, 135 (2003)
3. Bojan O. Boskovic, V. Stolojan, R.U.A. Khan, S. Haq, S. Ravi, P. Silva, *Nature Mat.* **1**, 165 (2002)
4. V. Rosato, M. Guillope, B. Legrand, *Philos. Mag.* **59**, 321 (1989)
5. R.P. Gupta, *Phys. Rev. B* **23**, 6265 (1981)
6. A.P. Amarillas, I.L. Garzón, *Phys. Rev. B* **54**, 10362 (1996)
7. I.L. Garzón, A.P.-Amarillas, *Phys. Rev. B* **54**, 11796 (1996).
8. I.L. Garzón et al., *Phys. Rev. Lett.* **81**, 1600 (1998)
9. K. Michaelian, N. Rendon, I.L. Garzón, *Phys. Rev. B* **60**, 2000 (1999)
10. J. Stanek, G. Mareš, H. Jaffrezic, H. Binczycka, *Phys. Rev. B* **52**, 8414 (1995)
11. F. Ding, K. Bolton, A. Rosen, *J. Vac. Sci. Technol. A* **22**, 1471 (2004)
12. F.A. Lindemann, *Phys. Z.* **11**, 609 (1910)
13. C.R.M. Wronski, *Br. J. Appl. Phys.* **18**, 1731 (1967)
14. S. Helveg, C.L. Cartes, J. Sehested, P.L. Hansen, B.S. Clausen, J.R.R. Nielsen, F.A. Pedersen, J.K. Nørskov, *Nature* **427**, 426 (2004)